CrossMark

Iterative Reconstructions in Reduced-Dose CT:
Which Type Ensures Diagnostic Image Quality in Young Oncology Patients?

Bastien Pauchard, MD, Kai Higashigaito, MD, Aicha Lamri-Senouci, MD, Jean-Francois Knebel, PhD, Dominik Berthold, MD, Francis Robert Verdun, PhD, Hatem Alkadhi, MD, Sabine Schmidt, MD

Rationale and Objectives: To compare adaptive statistical iterative reconstruction (ASIR) and model-based iterative reconstruction (MBIR) algorithms for reduced-dose computed tomography (CT).

Materials and Methods: Forty-four young oncology patients (mean age 30 ± 9 years) were included. After routine thoraco-abdominal CT (dose 100%, average $CTDI_{vol}$ 9.1 ± 2.4 mGy, range 4.4–16.9 mGy), follow-up CT was acquired at 50% (average $CTDI_{vol}$ 4.5 ± 1.2 mGy, range 2.2–8.4 mGy) in 29 patients additionally at 20% dose (average $CTDI_{vol}$ 1.9 ± 0.5 mGy, range 0.9–3.4 mGy). Each reduced-dose CT was reconstructed using both ASIR and MBIR. Four radiologists (two juniors and two seniors) blinded to dose and technique read each set of CT images regarding objective and subjective image qualities (high- or low-contrast structures), subjective noise or pixilated appearance, diagnostic confidence, and lesion detection.

Results: At all dose levels, objective image noise was significantly lower with MBIR than with ASIR ($P < 0.001$). The subjective image quality for low-contrast structures was significantly higher with MBIR than with ASIR ($P < 0.001$).

Reduced-dose abdominal CT images of patients with higher body mass index (BMI) were read with significantly higher diagnostic confidence than images of slimmer patients ($P < 0.001$) and had higher subjective image quality, regardless of technique.

Although MBIR images appeared significantly more pixilated than ASIR images, they were read with higher diagnostic confidence, especially by juniors ($P < 0.001$).

Conclusions: Reduced-dose CT during the follow-up of young oncology patients should be reconstructed with MBIR to ensure diagnostic quality. Elevated body mass index does not hamper the quality of reduced-dose CT.

Key Words: Computed tomography (MDCT); radiation exposure; radiographic image enhancement; image processing; computer-assisted; medical oncology.

© 2017 The Association of University Radiologists. Published by Elsevier Inc. This is an open access article under the CC BY-NC-ND license (http://creativecommons.org/licenses/by-nc-nd/4.0/).

INTRODUCTION

The number of computed tomography (CT) examinations has steadily increased worldwide along with the associated radiation exposure (1). Although the proportion of CT examinations among all imaging modalities using

X–rays is relatively low, their contribution to the overall annual medical radiation exposure is high (2,3). In particular, children and adolescents that are repetitively exposed to radiation are at increased stochastic risk of developing cancer (4,5). Thus, optimization of the technical parameters of CT is important to decrease the radiation dose.

During the last decade, CT machine vendors have introduced new methods of image reconstruction, mainly two types of iterative algorithms. By iterating the data several times, they provide images with less noise and higher contrast resolution than the conventional images obtained with filtered–back projection (FBP), which has been the conventional method of image reconstruction until recently (6). The first generation of iterative reconstruction (IR) techniques, namely adaptive statistical iterative reconstruction (ASIR) (ASIR, GE Healthcare, Milwaukee, WI, USA), was based on a mathematical algorithm applied to the raw data using FBP. Second-generation IR techniques are model–based iterative

reconstruction (MBIR). These methods do not blend with FBP and provide a greater noise reduction than first-generation IR methods. Thus, MBIR (VEO, GE Healthcare) enables a greater reduction of the associated radiation dose (7–12).

The potential for dose reduction using IR while preserving image quality has already been the subject of several publications (8,11,13–17), but only a few studies have analyzed both chest and abdominal CT images (10,18–24) and none have focused on young patients. As young patients represent the most radiosensitive population (25), they most urgently require an optimized radiation exposure, especially when they frequently undergo CT examinations, such as for follow-up of oncological disease.

The purpose of the present study was to compare the image quality of reduced-dose CT reconstructed by two types of IR (ie, the first-generation ASIR and second-generation MBIR) in routine follow-up of young oncology patients. We wanted to determine the exact potential of reducing dose without losing diagnostic information or the degree of confidence in the diagnosis. By including four readers in our image analysis (two juniors and two seniors), we investigated the influence of reduced-dose acquisition and image reconstruction artifacts on radiologists with various working experience.

MATERIALS AND METHODS

Patients

This single-center study was approved by our institutional ethics committee. All patients provided written informed consent before enrollment.

Over a period of 11 months (November 2013 to October 2014), we prospectively included all patients aged ≤45 years with known oncological disease who were referred to our department for follow-up CT at regular intervals according to their treatment schedule.

Exclusion criteria were the known contraindications for intravenous injection of iodinated contrast agents.

CT Examinations and Image Reconstruction

CT was performed on a 64-detector row CT machine (Discovery 750HD, GE Healthcare). The imaging protocol included either both the thorax and the abdomen/pelvis or the abdomen/pelvis only.

All patients underwent a first CT that was considered the reference examination. We performed a routine acquisition with 100% radiation dose exposure (120 kV, automatic tube current modulation in all three axes [SmartmA], noise index 25, $mA_{min} = 50$, $mA_{max} = 300$, table speed 55 mm/rotation [0.6 s], pitch 1.375, axial slice thickness/reconstruction interval 2.5 mm/2 mm). Reference CT images were reconstructed according to our routine default setting, including FBP and ASIR with 25% blending. We intravenously injected iodinated contrast

medium (Accupaque, Iohexol, 300 mgI/mL, GE Healthcare, volume in mL = bodyweight + 30 mL) at a flow rate of 3 mL/s.

Follow-up CT was performed with reduced-dose CT. The time interval depended on the oncological treatment schedule and ranged between 3 and 12 months. For reduced-dose CT, we divided our patients into two groups according to the number of abdominal phases we had to acquire. Patients with an arterial and portal-venous abdominal phase formed group 1, whereas patients with a portal-venous abdominal phase belonged to group 2. The number of abdominal phases depended on the type of underlying tumor and our oncological imaging protocol. The patients in group 1 underwent CT at 50% of the original dose and the patients in group 2 underwent CT at 50% of the original dose immediately followed by CT at 20% of the original dose. Each of these reduced-dose CT examinations was reconstructed with two different IR modalities, ASIR (50% blending) and MBIR (VEO, GE Healthcare) (Fig 1).

For all reconstructed axial images, a slice thickness of 2.5 and increment of 2 mm were used. The tube current was set with a fixed noise index of 25. Although the reconstruction duration of ASIR images is seconds, it is 40 minutes on average for MBIR images.

When we acquired the reduced-dose CT, we decreased the dose by dividing the dose-length product (DLP, in mGycm) and the CT dose index ($CTDI_{vol}$) of the reference CT examination by 2 (50%) and by 5 (20%), respectively. As the $CTDI_{vol}$ is independent of the patient's anatomical length and dose conversion coefficients, we consider it the most appropriate measure for quantifying dose reduction (7). Table 1 shows the overall radiation exposure of our patient population, expressed as $CTDI_{vol}$ and DLP.

Image Analysis

Five different groups of CT examinations were analyzed: the reference CT examinations (100% dose), the CT examinations acquired with 50% dose and reconstructed with ASIR and MBIR, and the CT examinations acquired at 20% dose reconstructed with ASIR and MBIR. Each CT examination was independently evaluated by four readers, including two seniors (KH, SS) with >5 years of experience in cross-sectional imaging and two juniors (BP, AL) with <5 years of experience in cross-sectional imaging. The readers reviewed images on a picture archiving and communication system workstation (Carestream Vue, version 11.4; Carestream Health, Rochester, NY, USA) and were blinded to the type of acquisition, data reconstruction, and dose. Moreover, during the image analysis the CT examinations were presented to each reader in a completely randomized order, because the IR technique and the applied dose totally varied from one CT examination to the other. Thus, none of the four readers knew what type of IR technique and which dose had been employed for a given CT examination, when he was evaluating the images.
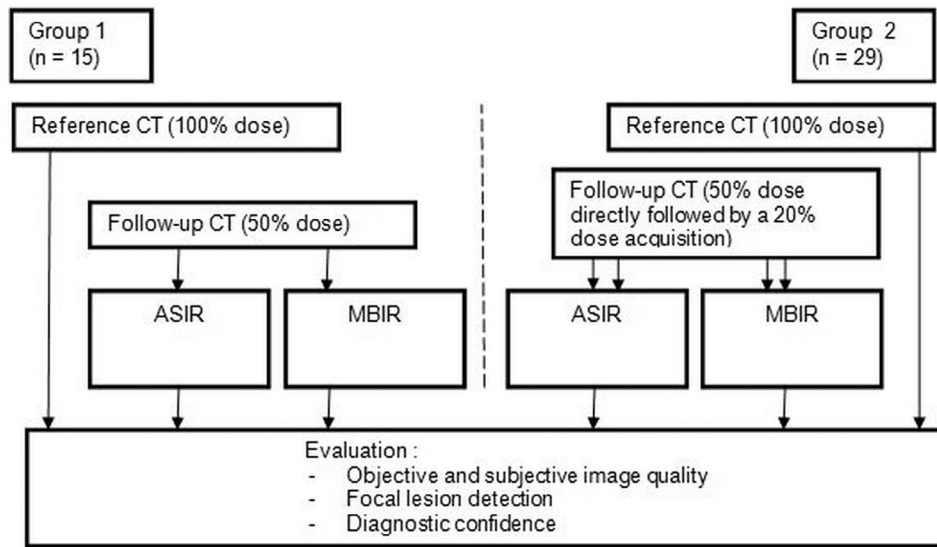
Figure 1. Flow chart of the imaging protocols for the two patient groups.

TABLE 1. Patients' Exposition Dose

Type of Examination	Reference CT (100% Dose)	Follow-up CT (50% Dose)	Follow-up CT (20% Dose)
Patients' CTDI$_{vol}$			
Abdominal CT ($n = 10$)	8.7 mGy (range 6.6–12.5 mGy)	4.4 mGy (range 3.1–6.2 mGy)	1.9 mGy (range 1.6–2.4 mGy)
Thoracoabdominal CT ($n = 34$)	9.2 mGy (range 4.4–17 mGy)	4.58 mGy (range 2.2–8.4 mGy)	1.9 mGy (range 0.9–3.4 mGy)
Total CTDI$_{vol}$	9.1 ± 2.4 mGy (range 4.4–16.9 mGy)	4.5 ± 1.2 mGy (range 2.2–8.4 mGy)	1.9 ± 0.5 mGy (range 0.9–3.4 mGy)
Patients' dose-length products (DLP)			
Abdominal CT ($n = 10$)	675.6 mGy × cm (range 367–998)	311.8 mGy × cm (range 194–448)	115.2 mGy × cm (range 77–155)
Thoraco-abdominal CT ($n = 34$)	730.5 mGy × cm (range 310–1302)	355.3 mGy × cm (range 149–580)	134.4 mGy × cm (range 53–232)
Total DLP	718.0 ± 225 mGy × cm (range 310–1302)	345.4 ± 102.5 mGy × cm (range 149–580)	131.1 ± 35.9 mGy × cm (range 53–232)

CT, computed tomography; CTDI, computed tomography dose index.

Objective Image Quality

For each CT examination, regardless of the type of IR, the average attenuation (in Hounsfield units) and standard deviation of attenuation were measured by placing a region of interest between 400 and 500 mm^2 in the right psoas muscle (below the kidneys and above the iliac crest). The standard deviation of attenuation was used to determine the objective image noise.

Subjective Image Quality

Subjective image quality was evaluated according to the commonly used visual grading analysis. The detection of high-contrast lesions was evaluated by testing the visibility of several small anatomical structures (15). Accordingly, the pericardium, the inter- or intramuscular septae of the thoracic wall, the adrenal glands, and the superficial inferior epigastric vessels were evaluated using a 5-point scale (1 = excellent visualization with well-defined margins, 2 = above average visibility but less well-defined margins, 3 = acceptable visibility but

ill-defined margins, 4 = suboptimal visibility with ill-defined margins, and 5 = unacceptable visualization without visualization of margins).

Low-contrast lesions were evaluated (15) by testing the visibility of the intrahepatic and intraportal veins to the segmental level, using a 5-point scale (1 = excellent image contrast, 2 = above average contrast, 3 = acceptable contrast, 4 = suboptimal contrast, and 5 = very poor contrast).

The overall subjective image noise and subjective pixilated blotchy appearance were evaluated separately for each thoracic and abdominal CT acquisition A 5-point scale was used for the image noise (1 = minimal image noise, 2 = less than average image noise, 3 = average image noise, 4 = above average image noise, and 5 = unacceptable image noise) and the pixilated blotchy appearance (1 = minimal pixilated blotchy appearance, 2 = less than average pixilated blotchy appearance, 3 = average pixilated blotchy appearance, 4 = above average pixilated blotchy appearance, and 5 = pixilated blotchy appearance). The pixilated blotchy appearance is a unique

feature resulting from the MBIR mode and appears on CT images as small steps at tissue interfaces. This may affect the sharpness of the anatomical structures upon visualization (10,15,26).

Finally, the overall diagnostic confidence of each thoracic and abdominal CT acquisition was evaluated using a 4-point scale (1 = fully confident, 2 = probably confident for diagnostic interpretation, 3 = confident only under limited conditions for visualization of abnormalities, and 4 = unacceptable).

Focal Lesion Detection

The visibility of focal parenchymal lesions (lung, liver, pancreas, spleen, and/or kidneys) measuring ≥6 mm at its largest diameter, and lymphadenopathies (supra- or infraclavicular, internal mammary, mediastinal, hilar, celiac, hepatic hilar, retroperitoneal, mesenteric and internal or external iliac sites) measuring ≥ 6 mm at its smallest diameter, was assessed using a 5-point scale (0 = no focal lesion ≥6 mm detected at the site to be evaluated, 1 = presence of ≥1 lesion with excellent visualization, 2 = presence of ≥1 lesion with above average visibility, 3 = presence of ≥1 lesion with suboptimal visibility, 4 = probable ≥1 lesion with very bad visibility, and 5 = impossible to analyze this lesion site). The standard of reference for these focal lesions detected on the reduced-dose images was a second follow-up CT acquired with the standard 100% dose 3–12 months after the reduced-dose CT.

Statistical Analysis

Statistical analyses were performed with the commercially available software R (R Core Team (2013), R: A language and environment for statistical computing, R Foundation for Statistical Computing, Vienna, Austria [https://www.r-project.org]). Data are presented as number and relative percentages. An unpaired t test was used to compare ASIR to VEO based on the different scores described previously. These t tests were applied to the reduced-dose CT examinations to highlight the relationship between the reconstruction algorithm and the dose. To investigate the deeper relationship of the evaluation scores, we introduced other dependent variables. These were the reader experiences (junior vs senior) and body mass index (BMI). We used analysis of variance to analyze these relationships using the two types of IR (ASIR vs MBIR) and dose reduction (50% vs 20%) as factors, as well as reader experiences (juniors vs seniors) in the first analysis and BMI (<median BMI vs ≥median BMI) in the second analysis. The possible correlation or interaction of the detection of focal lesions and lymphadenopathies with the degree of dose reduction and IR was evaluated by analysis of variance and the interobserver agreement between the readers was calculated with the kappa statistics and the ratings proposed by Fleiss (k < 0.4 = poor agreement; 0.4–0.75 = good agreement; >0.75 = excellent agreement).

All differences were considered significant at $P < 0.05$.

RESULTS

Patients and Examination Types

We included 44 patients (42 men, mean age 30 ± 9 years, range 17–44 years). Two patients had refused to participate during the inclusion period. The median weight was 81.8 kg (range 52–130 kg, mean 83.5 kg) and median BMI was 24.7 kg/m^2 (range 17.0–45.0 kg/m^2, mean 25.4 kg/m^2). The tumor types were testicular cancer ($n = 23$), sarcoma ($n = 14$), lymphoma ($n = 6$), and sacrococcygeal chordoma ($n = 1$). Follow-up CT was performed with a median delay of 5 months (mean 5.6 months, range 3–12 months) after the reference CT.

Fifteen (34.1%) of the patients belonged to the first group, and 29 (65.9%) patients comprised the second group (Fig 1). We finally performed 34 thoraco-abdominal and 10 abdominal CT examinations. We included 34 and 24 thoracic CT examinations acquired at a 50% and 20% dose, respectively, as well as 44 and 29 abdominal CT examinations acquired at a 50% and 20% dose, respectively, in the image analysis.

Evaluation of Reference CT Images and Comparison to ASIR and MBIR Images at 50% Dose

The results of the evaluation of the reference CT images are shown in Table 2 (first column) and correspond to the average results of the four readers, whose evaluation scores were analyzed together.

The average attenuation of the psoas muscle was similar on all image types. The mean objective image noise, measured by each reader using a region of interest placed in the psoas muscle, was lower on 50% dose MBIR images than the reference CT images (13.34 vs 18.68, $P < 0.001$).

For nearly all subjective parameters, the reference CT images were significantly better scored than the 50% dose images, regardless of the IR type (P values not shown). The only exception was the image noise, which was determined to be less prevalent on the 50% MBIR than on the reference CT images. However, this difference was significant for the abdomen only ($P < 0.001$). The pixilated appearance was determined to be absent on both the reference and the 50% ASIR images but prevalent on the 50% MBIR images ($P < 0.001$).

Comparison Between Reduced-Dose ASIR and MBIR Images

Table 2 (columns 2–7) summarizes the unpaired t test results of the reduced-dose image evaluation according to the type of IR by comparing the two 50% dose image types, that is, ASIR versus MBIR, and the two 20% dose image types with each other. The evaluation scores correspond to the results of the four readers taken together.

For both 50% and 20% dose, the objective image noise was lower on MBIR images than on ASIR images ($P < 0.001$).

TABLE 2. Evaluation Scores According to the Dose Reduction and the Reconstruction Algorithm (Four Readers)

CT Dose Reduction Type of IR	Reference 100%	50% ASIR	50% MBIR	P Value (t Test)	20% ASIR	20% MBIR	P Value (t Test)
Objective image quality (in Hounsfield units)							
Average density	67.66	67.95	67.27	0.40	69.52	67.30	0.06
Standard deviation	18.68	25.80	13.34	<0.001*	40.82	16.94	<0.001*
Subjective image quality							
High-contrast structures (5-point scale, 1 = best, 5 = worst)							
Pericardium	1.22	1.61	1.65	0.58	2.76	2.77	0.95
Chest wall	1.51	2.18	2.21	0.72	3.72	3.57	0.10
Adrenal glands	1.51	2.35	2.27	0.37	3.66	2.88	<0.001*
Superficial epigastric vessels	1.21	1.97	1.89	0.30	3.45	2.68	<0.001*
Low- contrast structures (5-point scale, 1 = best, 5 = worst)							
Portal veins	1.55	2.45	2.15	<0.001*	3.98	3.08	<0.001*
Hepatic veins	1.72	2.47	2.08	<0.001*	3.78	2.98	<0.001*
Subjective image noise/pixilated appearance (5-point scale, 1 = best, 5 = worst)							
Chest noise	1.28	2.41	1.21	<0.001*	3.48	2.06	<0.001*
Chest-pixilated appearance	1	1.01	2.27	<0.001*	1.48	2.62	<0.001*
Abdomen noise	1.64	3.14	1.32	<0.001*	3.07	1.65	<0.001*
Abdomen-pixilated appearance	1.01	1	2.64	<0.001*	1.72	3.08	<0.001*
Overall diagnostic confidence (4-point scale, 1 = best, 4 = worst)							
Chest	1	1.53	1.5	0.73	2.47	2.45	0.85
Abdomen	1.12	2.08	1.76	<0.001*	3.06	2.24	<0.001*

ASIR, adaptive statistical iterative reconstruction; CT, computed tomography; IR, iterative reconstruction; MBIR, model-based iterative reconstruction.

* Significant statistical differences.

The average attenuation of the psoas did not vary significantly, regardless of dose and technique.

Subjective evaluation of the high-contrast chest structures (pericardium, chest wall) did not find any significant difference between ASIR and MBIR, regardless of the percentage dose reduction. This was also true for the high-contrast structures of the abdomen at 50 % dose. However, when using a 20% dose, the high-contrast abdominal structures, that is, the adrenal glands and superficial epigastric vessels, were better assessed on MBIR images than on ASIR images ($P < 0.001$, Fig 2). The low-contrast structures, that is, the intrahepatic portal and hepatic veins, were better evaluated on MBIR images than on ASIR images, regardless of the percentage dose reduction ($P < 0.001$, Fig 3).

ASIR images were noisier than MBIR images for both thoracic and abdominal acquisitions, regardless of the percentage dose reduction ($P < 0.001$). Conversely, thoracic and abdominal MBIR images were considered more pixilated than ASIR images ($P < 0.001$).

Finally, the abdominal reduced-dose MBIR images were always evaluated with better diagnostic confidence than the abdominal reduced-dose ASIR images, regardless of the percentage dose reduction ($P < 0.001$). However, there was no different diagnostic confidence between the evaluation of reduced-dose ASIR and MBIR images of the chest.

In general, all readers read the 50% dose CT images with a higher diagnostic confidence than the 20% dose images, regardless of the IR technique.

Influence of BMI on Quality of ASIR and MBIR Images

To evaluate any possible influence of BMI, we divided our patients into two groups of approximately the same size by choosing the median BMI (24.7 kg/ m²) as a threshold. Thus, we obtained a group ($n = 23$) with a BMI ≤ 24.7 kg/m² and another group ($n = 21$) with a BMI > 24.7 kg/m². Their evaluation scores based on the two different IR techniques and dose are presented in Table 3, with the P values corresponding to the main effect of BMI. The evaluation scores correspond to the results of the four readers. Overall, the images of the group with higher BMI were evaluated better than those with the lower BMI, except for low-contrast structures. We also found differences between the two BMI groups that were independent of the two IR types and dose reductions.

The high-contrast structures (chest wall, adrenal glands, and superior epigastric veins) were better evaluated for the group with BMI > 24.7 ($P < 0.001$); only the pericardium showed a tendency ($P = 0.051$). Better evaluation scores were given to the low-contrast structures (hepatic and portal veins) of the high BMI patients, but the result was significant for the hepatic
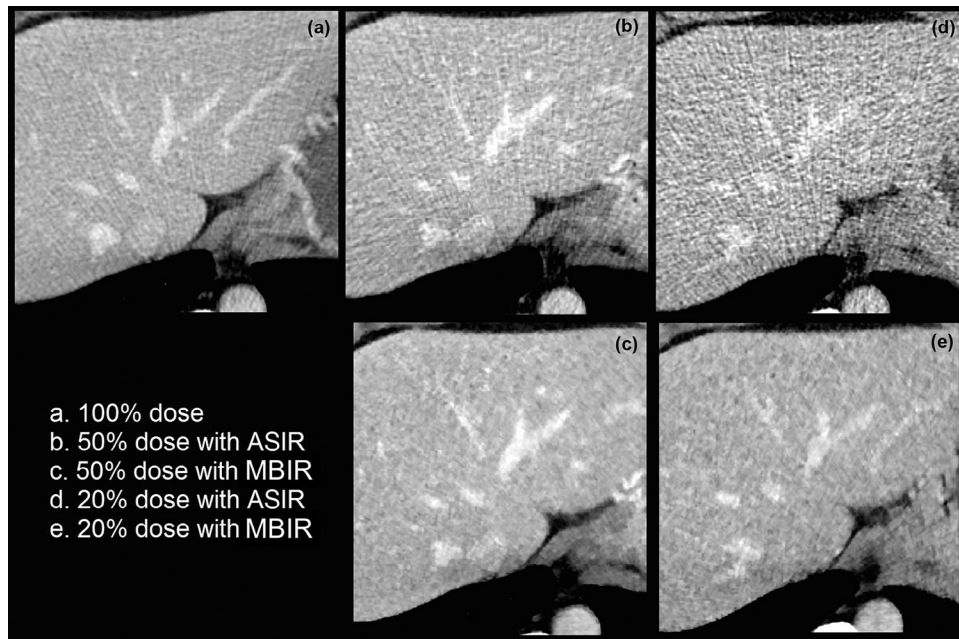
Figure 2. Side-by-side comparison of the intrahepatic veins for the reference 100% dose CT image **(a)** and two reconstruction algorithms and dose levels **(b–e)**. Note the excellent image contrast of the hepatic vessels on **(a)** and **(c)**, whereas image noise hampers the contrast on **(b)** and **(d)**. ASIR, adaptive statistical iterative reconstruction; MBIR, model-based iterative reconstruction.

veins only ($P < 0.001$; portal veins $P = 0.441$). The abdominal CT images were read with higher diagnostic confidence for the group with higher BMI, regardless of dose and technique ($P < 0.001$), but for the chest CT images a tendency was shown ($P = 0.067$).

Influence of Reader Experience on Evaluation of ASIR and MBIR Images

We found several differences between the scores of the juniors and seniors that were influenced by neither the two types of
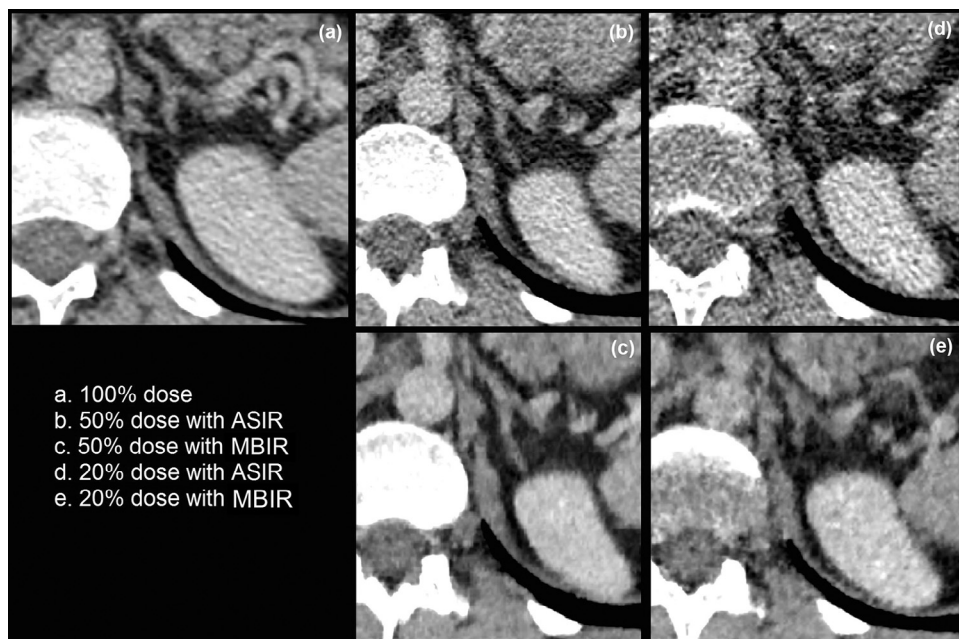

Figure 3. Visibility of the adrenal glands for the 100% dose CT image **(a)**, and two reconstruction algorithms and dose levels **(b–e)**. Note that the contours of the gland are better defined on the MBIR images **(c,e)** than on the corresponding ASIR images **(b,d)**. ASIR, adaptive statistical iterative reconstruction; MBIR, model-based iterative reconstruction.

TABLE 3. Influence of the BMI on the Image Evaluation (Four Readers)

Group of BMI	BMI ≤ 24.7		BMI >24.7		BMI ≤ 24.7		BMI >24.7		
Dose Reduction	50%	50%	50%	50%	20%	20%	20%	20%	
Type of IR	ASIR	MBIR	ASIR	MBIR	ASIR	MBIR	ASIR	MBIR	P Value[†]
Objective image quality (in Hounsfield units)									
Average density	70.98	70.67	64.62	63.55	74.70	72.29	64.68	62.64	<0.001*
Standard deviation	24.16	11.76	27.60	15.08	38.07	15.34	43.39	18.43	<0.001*
Subjective image quality									
High-contrast structures (5-point scale, 1 = best, 5 = worst)									
Pericardium	1.70	1.74	1.52	1.56	2.82	2.80	2.70	2.73	0.051
Chest wall	2.35	2.39	1.99	2.01	3.86	3.75	3.58	3.4	<0.001*
Adrenal glands	2.62	2.48	2.05	2.05	3.91	3.05	3.43	2.72	<0.001*
Superficial epigastric vessels	2.10	1.93	1.82	1.83	3.57	2.82	3.33	2.55	<0.001*
Low-contrast structures (5-point scale, 1 = best, 5 = worst)									
Portal veins	2.48	2.14	2.42	2.17	3.88	3.00	4.08	3.15	0.441
Hepatic veins	2.38	1.99	2.56	2.18	3.66	2.93	3.88	3.03	<0.001*
Subjective image noise/pixilated appearance (5-pointscale, 1 = best, 5 = worst)									
Chest noise	2.49	1.21	2.33	1.20	3.5	2.06	3.5	2.06	0.394
Chest-pixilated appearance	1.01	2.34	1	2.19	1.52	2.67	1.44	2.58	0.193
Abdomen noise	3.18	1.27	3.08	1.37	3.04	1.63	3.1	1.67	0.817
Abdomen-pixilated appearance	1	2.65	1	2.63	1.75	3.09	1.7	3.07	0.772
Overall diagnostic confidence (4-point scale, 1 = best, 4 = worst)									
Chest	1.59	1.55	1.45	1.44	2.52	2.49	2.42	2.42	0.067
Abdomen	2.16	1.84	1.99	1.68	3.05	2.36	3.07	2.13	<0.001*

ANOVA, analysis of variance; ASIR, adaptive statistical iterative reconstruction; BMI, body mass index; IR, iterative reconstruction; MBIR, model-based iterative reconstruction.

* Significant statistical differences.

[†] The given P value corresponds to the "main effect BMI" (calculated by means of ANOVA): it means that the result obtained by comparing the two different BMI groups is independent of the applied dose (50% or 20%) and the applied technique (ASIR vs VEO).

IR nor dose (Table 4). The P values given in Table 4 correspond to the main effect of the reader's experience. Except for the adrenal glands, the high-contrast structures were better evaluated by the seniors than the juniors (P < 0.001), whereas the juniors better scored the visibility of the low-contrast structures than the seniors (P < 0.001). The subjective image noise was graded worse by the juniors than by the seniors (P < 0.001), but the pixilated image appearance was evaluated similarly.

Generally, the reduced-dose images were evaluated with higher diagnostic confidence by the seniors than the juniors (P < 0.001), regardless of the type of IR.

Focal Lesion Detection According to Dose and Type of IR

The detection of focal organ lesions (P < 0.001, Fig 4) and thoraco-abdominal lymphadenopathies (P < 0.02, Fig 5) was significantly influenced by the dose (50% vs 20%), but not by the technique (ASIR vs MBIR). At 20% dose, MBIR images could slightly better demonstrate organ lesions (P = 0.67), but at 50% dose both IR techniques were similar. The detection of focal lesions in abdominal organs and thoraco-abdominal lymphadenopathies was not influenced by the radiologist's experience. The total number of detected lesions was 102, namely 87 lymphadenopathies and 25 focal

parenchymal lesions, as confirmed on the second follow-up CT acquired with the standard 100% dose 3–12 months after the reduced-dose CT. The interobserver agreement between the readers according to the IR technique and dose is demonstrated in Table 5. The mean and median kappa values were "good" for both techniques at 50% dose, whereas the values were "poor" for both techniques at 20% dose, without any significant difference between the two techniques.

DISCUSSION

As previously reported (6–9,13,14,16,18,19,21–23,26–29), IR algorithms enable a lower radiation dose for body CT acquisitions while preserving image quality. An evaluation of the 50% dose CT protocol by our four readers confirmed these findings, as diagnostic confidence was maintained and the subjective image quality of the reduced-dose images was still above average when compared to the reference, 100% dose images. Thus, in agreement with other authors (9,10,16,17,20,21,24,29), we think that routine follow-up in oncology patients with 50% reduced-dose CT is feasible, provided that IR algorithms are employed. We are the first to prospectively compare reduced-dose MBIR and ASIR images in young oncology patients, for whom the decrease in overall cumulative radiation exposure represents a major concern.

TABLE 4. Influence of the Readers' Experience on the Image Evaluation

Group of Reader	Juniors		Seniors		Juniors		Seniors		
Dose Reduction	50%	50%	50%	50%	20%	20%	20%	20%	
Type of IR	ASIR	VEO	ASIR	VEO	ASIR	VEO	ASIR	VEO	P Value[†]
Objective image quality (in Hounsfield units)									
Average density	68.48	67.28	67.41	67.26	69.71	66.71	69.33	67.89	0.08
Standard deviation	25.49	14	26.11	12.68	41.16	17.71	40.48	16.17	0.18
Subjective image quality									
High-contrast structures (5-point scale, 1 = best, 5 = worst)									
Pericardium	1.81	1.97	1.42	1.34	3.17	3.26	2.34	2.28	<0.001*
Chest wall	2.56	2.6	1.80	1.82	3.88	3.79	3.55	3.34	<0.001*
Adrenal glands	2.38	2.32	2.32	2.23	3.76	2.57	3.58	3.19	0.55
Superficial epigastric vessels	2.13	2.09	1.81	1.68	3.72	2.45	3.17	2.91	<0.001*
Low-contrast structures (5-point scale, 1 = best, 5 = worst)									
Portal veins	2.33	1.86	2.57	2.44	4.09	2.59	3.88	3.57	<0.001*
Hepatic veins	2.42	1.84	2.51	2.32	3.78	2.57	3.78	3.49	<0.001*
Subjective image noise/pixilated appearance (5-point scale, 1 = best, 5 = worst)									
Chest noise	2.64	1.41	2.19	1	3.54	3.12	3.42	1	<0.001*
Chest-pixilated appearance	1	2.31	1.01	2.23	1.96	2.18	1	3.06	0.52
Abdomen noise	3.57	1.60	2.7	1.03	2.31	2.19	3.83	1.10	<0.001*
Abdomen-pixilated appearance	1	2.69	1	2.59	2.43	2.55	1.02	3.60	0.11
Overall diagnostic confidence (4-point scale, 1 = best, 4 = worst)									
Chest	1.99	1.84	1.07	1.16	2.78	2.76	2.16	2.14	<0.001*
Abdomen	2.70	2.15	1.45	1.38	3.26	2.05	2.86	2.43	<0.001*

ANOVA, analysis of variance; ASIR, adaptive statistical iterative reconstruction; IR, iterative reconstruction.

* Significant statistical differences.

[†] The given *P* value corresponds to the "main effect reader" (calculated by means of ANOVA): it means that the result obtained by comparing the two different BMI groups is independent of the applied dose (50% or 20%) and the applied technique (ASIR vs VEO).
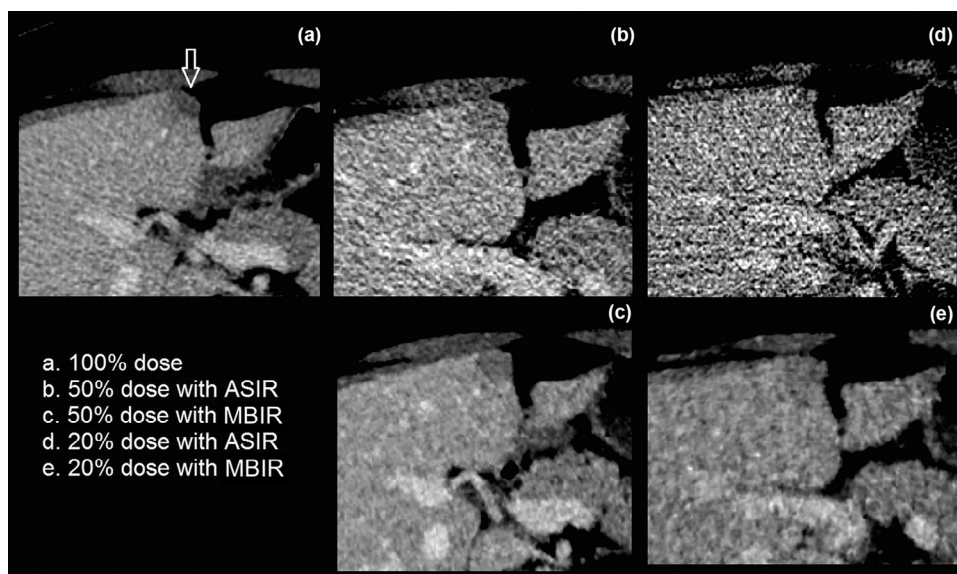

Figure 4. Side-by-side comparison of a subtle low-contrast liver lesion for the two iterative reconstruction algorithms and dose levels. A focal fatty area located within the hepatic parenchyma was detected on the 100% dose CT image **(a, arrow)**. Note that it is not confidently seen on the 50% dose MBIR image **(c)**, and is almost undetectable on both ASIR images **(b,d)** and on the 20% MBIR image **(e)**. ASIR, adaptive statistical iterative reconstruction; MBIR, model-based iterative reconstruction.
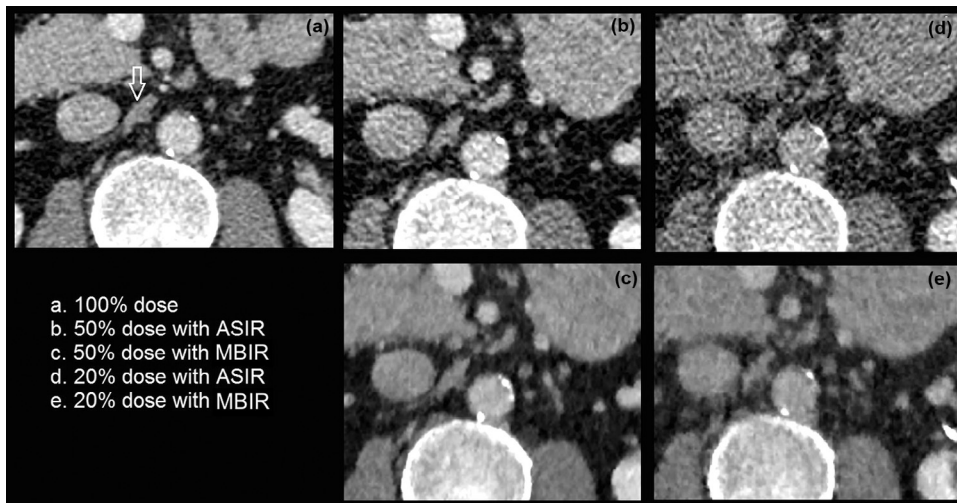
Figure 5. Side-by-side comparison of a retroperitoneal lymphadenopathy, detected on the 100% dose CT image **(a, arrow)** and the two iterative reconstruction algorithms and dose levels **(b–e)**. Although the lesion can be detected on each image, delineation is best on the 100% dose **(a)** and 50% dose **(c)** MBIR images. Image noise definitely hampers the contour sharpness on both reduced-dose ASIR images **(b,d)** and on the 20% dose MBIR image **(e)**. ASIR, adaptive statistical iterative reconstruction; MBIR, model-based iterative reconstruction.

TABLE 5. Interobserver Agreement Between the Four Readers for Detecting Focal Lesions on Reduced Dose CT Examinations

Kappa Values	Focal Parenchymal Lesions		Lymphadenopathies	
	Mean	Median	Mean	Median
ASIR 50%	0.59	0.61	0.51	0.51
VEO 50%	0.62	0.64	0.53	0.55
ASIR 20%	0.31	0.33	0.09	0
VEO 20%	0.33	0.37	0.031	0.01

ASIR, adaptive statistical iterative reconstruction; CT, computed tomography.

Our study and others revealed that, in reduced-dose CT examinations, MBIR better maintains diagnostic image quality than ASIR (9,11,18). This difference is obtained mainly because of the higher noise-reduction capabilities of MBIR. In addition to modeling photon and noise statistics, the MBIR algorithm takes into account specific hardware details, such as X-ray focal spot size, detector size, and image voxel shape and size (7,8,15). Thus, our results confirm the significantly less objective image noise on MBIR images compared to ASIR images.

As the objective image noise naturally increases as dose decreases, the noise difference between MBIR and ASIR becomes even more pronounced as dose exposure decreases. Currently, reduced-dose acquisitions represent a common strategy for CT follow-up in young oncology patients because follow-up may be lifelong (18). Therefore, the MBIR algorithm should definitely be the preferred option in these patients. In routine examinations not acquired in the emergency setting, the long

computational time necessary for reconstructing MBIR images (8,11) may not be relevant.

IR algorithms are mainly based on denoising, but extensive noise reduction does not necessarily lead to better image quality. We need to be aware of the distinct texture of MBIR images: the blotchy, pixilated, step-like appearance at tissue interfaces. This "pixelization" naturally increases as the dose decreases and is generally far more pronounced on MBIR images than on ASIR images at the same dose (7). This so-called "oversmoothing" is because of aggressive noise reduction (10,14,15) and needs to be taken into account separately when evaluating image quality. In our study, as in others (15), the blotchy pixilated image appearance did not compromise subjective image quality or the diagnostic performance of our reduced-dose images, as proven by the better scores for MBIR images than for ASIR images at each dose level.

Rarely (10,18–24), the quality of reduced-dose chest and abdomen images has been evaluated together. Although the diagnostic confidence of our readers generally decreased as the dose decreased, it always remained significantly higher for abdominal MBIR images than for the corresponding ASIR images. In particular, juniors had significantly less confidence than the seniors in the very noisy ASIR images acquired at 20% dose. The experience and familiarity of seniors reading noisy images explain this difference between the two reader groups. A certain amount of noise is usually present on CT images when they are reconstructed with FBP only, because this algorithm assumes noise-free projection data (10). In contrast, diagnostic confidence for chest images did not depend on the IR algorithm. As reported by Meyer et al., the noise reduction obtained by IR algorithms strongly depends on the tissue region considered (21). Therefore, organs with physiological noise, such as the lungs, are less affected by changes in image texture. Unlike in the abdomen, inherent contrast

and low attenuation in lung parenchyma enable the tolerance of image noise and substantial dose reduction (14).

Clinical applications with inherent high-contrast abnormalities, such as renal calculi, permit larger dose reductions without compromising image quality than low-contrast tasks (30), regardless of the IR technique (29). Accordingly, our study revealed no differences in subjective image quality between MBIR and ASIR for thoracic high-contrast structures, regardless of dose reduction, or for the abdominal high-contrast structures (adrenal glands, superficial epigastric vessels) at 50% dose. However, the latter were significantly better evaluated at 20% dose MBIR images than on ASIR images, as previously shown by Fontarensky et al., who evaluated MBIR at the same dose reduction for renal calculi (11). In contrast, the subjective image quality of our low-contrast structures was significantly higher on MBIR images than on corresponding ASIR images, regardless of dose and reader experience. Therefore, although the IR algorithm does not significantly preserve low-contrast detectability as the dose decreases (29), we agree with previous groups that demonstrate better low-contrast detectability with MBIR techniques than with statistical–based IR algorithms, such as ASIR, at the same dose level (6,30).

Finally, reduced-dose abdominal images of our patients with higher BMI were read with significantly higher diagnostic confidence than those of slimmer patients, and had higher scores for subjective quality, regardless of IR type and dose reduction, which were consistent with previous results (11,12). The scores for the chest images showed the same tendency. As we used automatic tube current modulation in the reference CT, the CTDI$_{vol}$ of our patients with higher BMI was always slightly higher than that of patients with lower BMI. In addition, small interstitial fat planes in more obese patients may allow better delineation of visceral organs and muscles than in slim patients, facilitating the analysis of reduced-dose images. Thus, dose reduction should be based on young age and length of necessary CT follow-up in young patients, rather than individual BMI.

According to our results, focal lesion detection was significantly influenced by dose rather than IR technique. On our 20% CT images, the detectability of liver lesions was drastically reduced (Fig 4). This finding was confirmed by Vardhanabhuti et al., who evaluated a similar dose (CTDIvol 2.3 mGy) (8) and by Padole et al. who evaluated even lower doses (CTDIvol 1.3 mGy) (26) with MBIR reconstructions. Pickhardt et al. reported a significantly higher rate of focal lesion detection on low-dose MBIR images compared to corresponding ASIR images (9), but this was not confirmed by our results. We believe that with too drastic dose reductions (≥80%), the smoothing and pixilated blotchy appearance inherent in MBIR images may not allow depiction of small hypoattenuating liver lesions (Fig 4) any more, thus dissimulating possible relevant clinical findings, especially in patients with high BMI.

According to recent publications, radiation dose settings and iterative reconstruction algorithms at multidetector row CT may significantly affect the quantitative imaging features of liver lesions, lung nodules, and renal stones (31), or even the size of vessels (32). In particular, with reduced-dose MBIR images a lesion volume may be differently estimated because of the nonlinear nature of this IR mechanism compared to 100% dose FBP reconstructed CT images (31). Therefore, one needs to be careful with size measurements when implementing MBIR reduced-dose CT examinations. However, the latter may not be an important issue when dealing with routine follow-up CT examinations, for which we consecutively and steadily apply the same technical parameters.

Our study has several limitations. First, the two reduced-dose CT acquisitions were performed sequentially after intravenous injection of contrast medium. Thus, 15 (34.1%) patients, in whom the oncological protocol required an arterial abdominal phase before the portovenous acquisition, did not undergo a supplementary 20% dose CT. In addition, visceral structures may have been affected by a slightly different contrast opacification on the 20% dose CT images than the 50% dose CT images, although the delay between acquisitions was kept as short as possible. Secondly, MBIR images appear quite differently from ASIR images, so it was impossible to completely blind the readers. Nevertheless, we anonymized and randomized the different image sets under evaluation. Finally, the evaluation of subjective image quality is, by definition, limited to the subjective and instant impression of the perceived images. We tried to compensate for this by including a considerable number of readers with different daily working experience.

In conclusion, our study shows the diagnostic superiority of MBIR compared to ASIR for reduced-dose body CT in young oncology patients. Therefore, in this dose-sensitive patient population, 50% dose MBIR CT examinations should be considered for follow-up. The analysis of reduced-dose abdominal images remains more challenging than that of corresponding chest images, because of the limited low-contrast detectability inherent in each type of IR.

REFERENCES

1. Brenner DJ, Hall EJ. Computed tomography–an increasing source of radiation exposure. N Engl J Med 2007; 357:2277–2284.
2. Samara ET, Aroua A, Bochud FO, et al. Exposure of the Swiss population by medical X-rays: 2008 review. Health Phys 2012; 102:263–270.
3. Hara AK, Paden RG, Silva AC, et al. Iterative reconstruction technique for reducing body radiation dose at CT: feasibility study. AJR Am J Roentgenol 2009; 193:764–771.
4. Pearce MS, Salotti JA, Little MP, et al. Radiation exposure from CT scans in childhood and subsequent risks of leukaemia and brain tumors: a retrospective study. Lancet 2012; 380:499–505.
5. Mathews JD, Forsythe AV, Brady Z, et al. Cancer risk in 680 000 people exposed to computed tomography scans in childhood or adolescence: data linkage study of 11 million Australians. BMJ 2013; 346:346. f2360.
6. Patino M, Fuentes JM, Singh S, et al. Iterative reconstruction techniques in abdominopelvic CT: technical concepts and clinical implementation. AJR Am J Roentgenol 2015; 205:W19–W31.
7. Willemink MJ, de Jong PA, Leiner T, et al. Iterative reconstruction techniques. Eur Radiol 2013; 23:1623–1631.
8. Vardhanabhuti V, Riordan RD, Mitchell G, et al. Image comparative assessment using iterative reconstructions. Invest Radiol 2014; 49:209–216.
9. Pickhardt J, Lubner MG, Kim DH, et al. Abdominal CT with model-based iterative reconstruction (MBIR): initial results of a prospective trial

comparing ultralow-dose with standard-dose. AJR Am J Roentgenol 2012; 199:1266–1274.

10. Ploussi A, Alexopoulou E, Economopoulos N, et al. Patient radiation exposure and image quality evaluation with the use of idose[4] iterative reconstruction algorithm in chest-abdomen-pelvis CT examinations. Radiat Prot Dosimetry 2014; 158:399–405.

11. Fontarensky M, Alfidja A, Perignon R, et al. Reduced radiation dose with model-based iterative reconstruction versus standard dose with adaptive statistical iterative reconstruction in abdominal CT for diagnosis of acute renal colic. Radiology 2015; 276:156–166.

12. Gervaise A, Naulet P, Beuret F, et al. Low-dose CT with automatic tube current modulation, adaptive statistical iterative reconstruction, and low tube voltage for the diagnosis of renal colic: impact of body mass index. AJR Am J Roentgenol 2014; 202:553–560.

13. Prakash P, Kalra MK, Kambadakone AK, et al. Reducing abdominal CT radiation dose with adaptive statistical iterative reconstruction technique. Invest Radiol 2010; 45:202–210.

14. Padole A, Ali Khawaja RD, Kalra MK, et al. CT radiation dose and iterative reconstruction techniques. AJR Am J Roentgenol 2015; 204:W384–W392.

15. Singh S, Kalra MK, Hsieh J, et al. Abdominal CT: comparison of adaptive statistical iterative and filtered back projection reconstruction techniques. Radiology 2010; 257:373–383.

16. May MS, Wüst W, Brand M, et al. Dose reduction in abdominal computed tomography. Invest Radiol 2012; 46:465–470.

17. Schabel C, Fenchel M, Schmidt B, et al. Clinical evaluation and potential radiation dose reduction of the novel sinogram-affirmed iterative reconstruction technique (SAFIRE) in abdominal computed tomography angiography. Acad Radiol 2013; 20:165–172.

18. Hérin E, Gardavaud F, Charadia M, et al. Use of model-based iterative reconstruction (MBIR) in reduced-dose CT for routine follow-up of patients with malignant lymphoma: dose savings, image quality and phantom study. Eur Radiol 2015; 25:2362–2370.

19. Kalmar PI, Quehenberger F, Steiner J, et al. The impact of iterative reconstruction on image quality and radiation dose in thoracic and abdominal CT. Eur J Radiol 2014; 83:1416–1420.

20. Arapakis I, Efstathopoulos E, Tsitsia V, et al. Using "iDose[4]" iterative reconstruction algorithm in adults' chest–abdomen–pelvis CT examinations: effect on image quality in relation to patient radiation exposure. Br J Radiol 2014; 87:20130613.

21. Meyer M, Klein SA, Brix G, et al. Whole-body CT for lymphoma staging: feasibility of halving radiation dose and risk by iterative image reconstruction. Eur J Radiol 2014; 83:315–321.

22. Gonzalez-Guindalini FD, Ferreira Botelho MP, Töre HG, et al. MDCT of chest, abdomen, and pelvis using attenuation-based automated tube voltage selection in combination with iterative reconstruction: an intrapatient study of radiation dose and image quality. AJR Am J Roentgenol 2013; 201:1075–1082.

23. Karpitschka M, Augart D, Becker H-C, et al. Dose reduction in oncological staging multidetector CT: effect of iterative reconstructions. Br J Radiol 2013; 86:20120224.

24. Smith E, Dillman JR, Goodsitt MM, et al. Model-based iterative reconstruction: effect on patient radiation dose and image quality in pediatric body CT. Radiology 2014; 270:526–534.

25. Brenner DJ, Doll R, Goodhead DT, et al. Cancer risks attributable to low doses of ionizing radiation: assessing what we really know. Proc Natl Acad Sci USA 2003; 100:13761–13766.

26. Padole A, Singh S, Lira D, et al. Assessment of filtered back projection, adaptive statistical and model-based iterative reconstruction for reduced dose abdominal computed tomography. J Comput Assist Tomogr 2015; 39:462–467.

27. Martinsen ACT, Saether HK, Hol PK, et al. Iterative reconstruction reduces abdominal CT dose. Eur J Radiol 2012; 81:1483–1487.

28. Thomas P, Hayton A, Beveridge T, et al. Evidence of dose saving in routine CT practice using iterative reconstruction derived from a national diagnostic reference level survey. Br J Radiol 2015; 88:20150380.

29. Klink T, Obmann V, Heverhagen J, et al. Reducing CT radiation dose with iterative reconstruction algorithms: the influence of scan and reconstruction parameters on image quality and CTDI$_{vol}$. Eur J Radiol 2014; 83:1645–1654.

30. Ehman EC, Yu L, Manduca A, et al. Methods for clinical evaluation of noise reduction techniques in abdominopelvic CT. Radiographics 2014; 34:849–862.

31. Solomon J, Mileto A, Nelson RC, et al. Quantitative features of liver lesions, lung nodules, and renal stones at multi-detector row CT examinations. Radiology 2016; 279:185–194.

32. Minhas A, Patel S, Kazerooni EA, et al. Iterative reconstruction results in larger computed tomography measurements of iliofemoral artery diameter in patients referred for transcatheter aortic valve replacement. J Comput Assist Tomogr 2016; 40:773–776.